ISSN 0967-859X
THE SOCIETY FOR EARTHQUAKE AND CIVIL ENGINEERING DYNAMICS

SECED NEWSLETTER

Volume 26 No 2
August 2015

In this issue

The Dynamics of Rocking Isolation

Nicos Makris
Division of Structures, Civil Engineering, University of Central Florida, Orlando, FL 32816
Office of Theoretical and Applied Mechanics, Academy of Athens, GR-106 79

Abstract

The uplifting and rocking of slender, free-standing structures when subjected to ground shaking may limit appreciably the seismic moments and shears that develop at their base. This high-performance seismic behaviour is inherent in the design of ancient temples that consist of slender, free-standing columns which support freely heavy epistyles together with the even heavier frieze atop. While the ample seismic performance of rocking isolation has been documented with the through-the-centuries survival of several free-standing ancient temples; and careful post-earthquake observations in Japan during the 1940's suggested that the increasing size of slender free-standing tombstones enhances their seismic stability; it was Housner (1963) who half a century ago elucidated a size-frequency scale effect and explained that there is a safety margin between uplifting and overturning and as the size of the column or the frequency of the excitation increases, this safety margin increases appreciably to the extent that large free-standing columns enjoy ample seismic stability. This article revisits the important implications of this post-uplift dynamic stability and explains that the enhanced seismic stability originates from the difficulty of mobilizing the rotational inertia of the free-standing column. As the size of the column increases, the seismic resistance (rotational inertia) increases with the square of the column size; whereas, the seismic demand (overturning moment) increases linearly with size. The same result applies to the articulated rocking frame given that its dynamic rocking response is identical to the rocking response of a solitary free-standing column with the same slenderness; yet larger size. The article concludes that the concept of rocking isolation by intentionally designing a hinging mechanism that its seismic resistance originates primarily from the mobilization of the rotational inertia of its members is a unique seismic protection strategy for large, slender structures not just at the limit-state but also at the operational state.

Editor's note: On March 15th, Professor Nicos Makris gave a presentation on "The Dynamics of Rocking Isolation" at City University, London. The talk was organised jointly by the City University's Research Centre for Civil Engineering Structures (RCCES), and SECED. Professor Makris kindly provided this detailed summary of the presentation and his work on rocking structures. Readers interested in more information on the topic may like to follow up on selections from the extensive references section of this article, as well as Dr DeJong's article from July 2014's SECED newsletter.

1. Introduction

The design of most structural framing systems is based on three basic concepts which are deeply rooted in modern structural engineering. The first concept is that of creating statically indeterminate (redundant) framing systems. When an "indeterminate" structure is loaded by strong lateral loads and some joints develop plastic hinges, there is enough redundancy in the system so that other joints maintain their integrity. In this way, recentring of the structures is achieved to some extent and stability is ensured. The second concept, known as ductility, is the ability of the structure to maintain sufficient strength at large deformations. In this way, even in the event of excessive lateral loads that may convert all joints to plastic hinges, all modern seismic codes demand that these hinges shall develop sufficient ductility so that collapse is prevented; however, in this case the structure may experience appreciable permanent displacements. The third concept that dominates modern structural engineering is that of positive stiffnesses. When a structure behaves elastically, forces and deformations are proportional. When yielding is reached the forces are no longer proportional to the deformations; however, in most cases the stiffnesses at any instant of the deformation history of the structure remain positive—that is if some force is needed to keep the structure away from equilibrium at some displacement, then a larger force is needed to keep the structure away from equilibrium at a larger displacement. Fig. 1 (left) illustrates the deformation pattern of a moment-resisting, fixed-base frame when subjected to a lateral load capable of inducing yielding at the joints. The force-deformation curve (P-u) is nonlinear; nevertheless, the lateral stiffness of the system remains positive at all times.

Fig. 1 (right) illustrates the deformation pattern of a free-standing rocking frame (two free-standing rigid columns capped with a freely supported rigid beam) when subjected to a lateral load capable of inducing uplifting of the columns. The force-displacement relationship (P-u) of the rocking frame shown at the bottom of Fig. 1 (right) indicates that the articulated system has infinite stiffness until uplift is induced and once the four-hinge frame is set into rocking motion, its restoring force decreases monotonically, reaching zero when the rotation of the column $\theta = \alpha = \arctan(b/h)$. Accordingly, the free-standing rocking frame shown in Fig. 1 (right) is a four-hinge mechanism that exhibits negative lateral stiffness. Fig. 1 indicates that while most modern structural engineers are trained to design statically indeterminate structures that exhibit positive stiffnesses and hopefully sufficient ductility (Fig. 1 left); ancient builders were designing entirely different structural systems—that is articulated mechanisms that exhibit negative stiffnesses and low damping (Fig. 1 right).

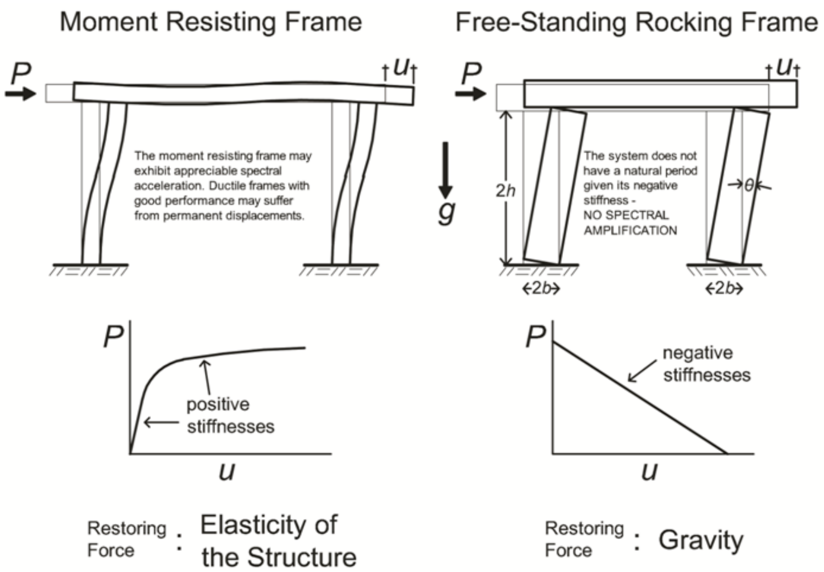

Figure 1: The fundamental difference in the behaviour of a traditional moment-resisting frame (left) and a rocking frame with free-standing columns which are allowed to rock (right).

Figure 2: View of the Temple of Apollo in Corinth, Greece. Its monolithic, free-standing columns support massive epistyles and the frieze atop, and the entire rocking frame remains standing for more than 2500 years in a region with high seismicity.

What is remarkable about these "unconventional" articulated structures is that they have endured the test of time by surviving several strong seismic motions during their 2.5 millennia life. For instance, Fig. 2 shows a view of the late archaic Temple of Apollo in Corinth, Greece (Powell, 1905).

The unparalleled seismic performance of the free-standing rocking frames shown in Fig. 2 is due to the very reason that they are articulated mechanisms. In this way: (a) given their negative stiffnesses they are not subject to any resonance, (b) recentring (elimination of any permanent displacement) is achieved unconditionally with gravity; and (c) the rocking frames, while slender and emblematic, are large in size to the extent that their rotational inertia, when mobilized, is enough to resist the 2500 years seismic hazard.

Analytical studies on the seismic response of slender, free-standing columns have been presented as early as in 1885 by Milne (1885) in an effort to estimate levels of ground shaking. His reasoning is entirely within the context of an equivalent static analysis and by taking moment equilibrium about the imminent pivoting point, he concludes that when the ground acceleration, $\ddot{u}_g$, exceeds the value of $g \times$ (width/height), the column overturns. Four decades after Milne's work, Kirkpatrick (1927) published a remarkable paper on the seismic stability of rocking columns. His work brings forward the two key quantities other than the peak ground acceleration that are responsible for the stability of a slender, free-standing column: (a) the size of the column which enters the equations via the moment of inertia; and (b) the duration of the period of the excitation. Kirkpatrick (1927) after correctly deriving the minimum acceleration amplitude of a harmonic excitation that is needed to overturn a free-standing column with a given size and slenderness, proceeds by presenting the first minimum-acceleration overturning spectrum (Fig. 6 of Kirkpatrick's 1927 paper) and shows that as the period of the excitation decreases, a larger acceleration is needed to overturn a free-standing column. While P. Kirkpatrick worked in Hawaii, it appears that his contributions were not known in Japan. Nevertheless, in the late 1940's Ikegami and Kishinouye published two important papers, one following the December 21, 1946 Nankai Earthquake (Ikegami and Kishinouye, 1947) and the other following the December 26, 1949 Imaichi Earthquake (Ikegami and Kishinouye, 1950). These two papers came to confirm Kirkpatrick's theoretical findings on the rocking response of free-standing columns; since they indicate that the static threshold, $g \times$ (width/height), is too low and is not able to explain the observed stable response of more slender; yet, larger tombstones. In their own words Ikegami and Kishinouye (1950) write "*In our field investigations, we often met with cases where gravestones had not overturned because of their large dimensions in spite of the small value of the ratio between width and height*".

About a decade later Muto et al. (1960) build upon the work of Ikegami and Kishinouye (1947; 1950) and showed explicitly that the dynamic response of a rocking column is governed by a negative stiffness; therefore, its free-vibration response is not harmonic; rather it is described by hyperbolic sines and cosines.

The pioneering work of Kirkpatrick (1927) in association with the systematic work conducted in Japan on rocking and overturning during the first-half of the 20th century matured the knowledge on this subject to the extent that Housner (1963), after introducing the concept of pulse-excitations, elucidated a size-frequency scale effect that explained why (a) the larger of two geometrically similar columns can survive the excitation that will topple the smaller column and (b) out of two same acceleration amplitude pulses, the one with longer duration is more capable of inducing overturning. While the exact dynamic rocking response of the free-standing slender column turns out to be rather complex, the following section offers a qualitative explanation of the size-frequency scale effect initially identified by Kirkpatrick (1927) and made popular to the earthquake engineering community by Housner (1963).

2. A notable limitation of the equivalent static lateral force analysis

2.1 Seismic resistance of free-standing columns under "Equivalent Static" lateral loads

Consider a free-standing rigid column with size $R = \sqrt{b^2 + h^2}$ and slenderness $b/h = \tan\alpha$ as shown in Fig. 3 (left). Let us first assume that the base of the column is moving (say to the left) with a "slowly" increasing acceleration, $\ddot{u}_g$ (say a very long-duration acceleration pulse which allows for an equivalent static analysis). Uplift of the column (hinge formation) happens when the seismic demand (overturning moment) = $m\ddot{u}_g h$ reaches the seismic resistance (recentring moment) = mgb. When uplifting is imminent, "static" moment equilibrium of the column about the pivoting point O gives

$$m\ddot{u}_g h = mgb \qquad \text{or} \qquad \ddot{u}_g = g\frac{b}{h} = g\tan\alpha \tag{1}$$

Eq. (1), also known as West's formula (Milne, 1885; Kirkpatrick ,1927), shows that the column <b, h> will uplift when $\ddot{u}_g \geq g\tan\alpha$. Now, given that this is a "quasistatic" lateral inertial loading, the inertia moment due to the nearly zero rotational accelerations of the columns is negligible ($\ddot{\theta}(t) = 0$). Once uplift has occurred, the rocking column experiences a positive rotation, $\theta(t)$; therefore, the seismic demand is $m\ddot{u}_g R\cos(\alpha - \theta(t))$; while the seismic resistance is merely $mgR\sin(\alpha - \theta(t))$ since $\ddot{\theta}(t) = 0$. For $\theta > 0$, the resistance of the rocking column upon uplifting under quasistatic lateral loading is $\tan(\alpha - \theta(t))$ which is smaller than $\tan\alpha$. Accordingly, once the column uplifts, it will also overturn. From this analysis one concludes that under quasistatic lateral loading the stability of a free-standing column depends solely on its slenderness ($g\tan\alpha$) and is independent to the size ($R = \sqrt{b^2 + h^2}$).

2.2 Seismic resistance of free-standing columns subjected to dynamic loads

In reality, earthquake shaking, $\ddot{u}_g$, is not a quasistatic loading and once uplifting has occurred the column will experience a finite rotational acceleration ($\ddot{\theta}(t) \neq 0$). In this case, dynamic moment equilibrium gives

$$-m\ddot{u}_g(t)R\cos[\alpha - \theta(t)] = I_o\ddot{\theta}(t) + mgR\sin[\alpha - \theta(t)] \qquad \theta > 0 \tag{2}$$

where I_o is the rotational moment of inertia of the column about the pivot point at the base—a quantity that is proportional to the square of the size of the column, R. As an example for rectangular columns, $I_o = (4/3)mR^2$, and Eq. (2) simplifies to

$$-\ddot{u}_g(t)R\cos[\alpha - \theta(t)] = \frac{4}{3}R^2\ddot{\theta}(t) + gR\sin[\alpha - \theta(t)] \qquad \theta > 0 \tag{3}$$

Eq. (3) indicates that when a slender free-standing column is set into rocking motion the seismic demand (overturning seismic moment) is proportional to R (first power of the size); whereas, the seismic resistance (opposition to rocking) is proportional to R^2 (second power of the size).

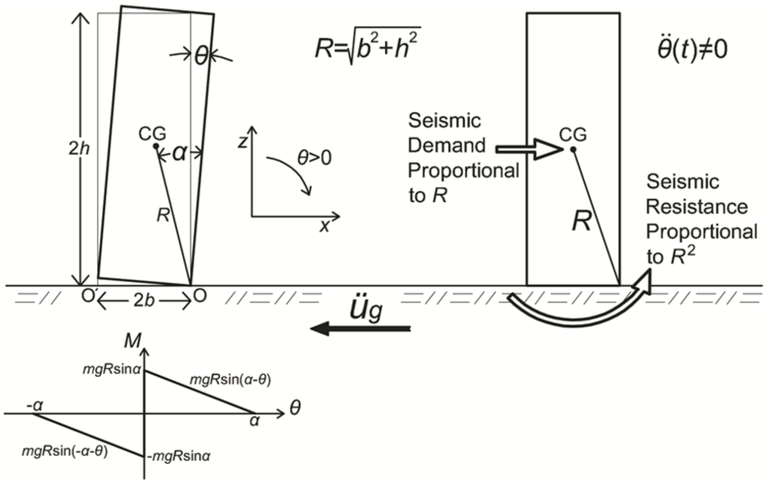

Figure 3: Left: Geometric characteristics of a free-standing rocking column together with its moment rotation diagram. Right: During earthquake shaking which sets the column in rocking motion ($\ddot{\theta}(t) \neq 0$) the seismic resistance is proportional to R^2; while, the seismic demand is proportional to R. Consequently, when a free-standing column is sufficiently large it can survive large horizontal accelerations even if it is very slender.

Consequently, Eq. (3) dictates that regardless how slender a column is (small α) and how intense the ground shaking, $\ddot{u}_g$, is (seismic demand), when a rotating column ($\ddot{\theta}(t)$ = finite) is large enough, the second power of R in the right-hand-side (seismic resistance) can always ensures stability. Simply stated, Housner's (1963) size effect is merely a reminder that a quadratic term eventually dominates over a linear term regardless of the values of their individual coefficients.

Fig. 3 (right) shows schematically the relations with the size R of the seismic demand (linear relation) and the seismic resistance (quadratic relation). From its very conception the "equivalent static lateral force analysis" is not meant to deal with any rotational acceleration term; therefore, its notable failure to capture the seismic stability (resistance) of tall free-standing structures. Simply stated, ancient builders were designing structures such that their seismic resistance originates primarily from the mobilization of their rotational inertia—a truly dynamic design. It is worth emphasizing that slender rocking structures have moderate strength (uplifting initiates when $\ddot{u}_g > g\,(b/h) = g\tan\alpha$), and negative stiffness; whereas, damping during rocking happens only at the instant of impact; therefore, the ductility of these systems is zero. Table 1 compares the basic design concepts together with the main response-controlling quantities that are associated with: (a) the traditional earthquake resistant (capacity) design; (b) seismic isolation; and (c) rocking isolation.

It is worth noting that during the last decade there has been a series of publications which aim to direct the attention of engineers to the unique advantages associated with allowing structures to uplift. The underlying concept in this class of publications is the intentional generation of uplifting mechanisms in traditional moment resisting frames (Ajrab et al., 2004; Harden et al., 2006; Kawashima et al., 2007; Gajan and Kutter, 2008; Anastasopoulos et al.,

Table 1: Basic design concepts and response-controlling quantities associated with: (a) the traditional earthquake resistant (capacity) design; (b) seismic isolation; and (c) rocking isolation.

	Traditional Earthquake Resistant Design (Moment Resisting Frames, Braced Frames)	Seismic Isolation	Rocking Isolation
Strength	Moderate to appreciable $\ddot{u}_g^y = \frac{Q}{m} = 0.10g\text{–}0.25g$	Low $\ddot{u}_g^y = \frac{Q}{m} = 0.03g\text{–}0.09g$	Moderate $\ddot{u}_g^{up} = g\frac{b}{h} = g\tan\alpha$
Stiffness	Positive and variable due to yielding	Positive, low and constant	Negative and constant
Ductility	Appreciable $\mu = 3\text{–}6$	Very large / immaterial* LRB†: $\mu = 10\text{–}30$ CSB‡: $\mu = 1000\text{–}3000$	Zero
Damping	Moderate	Moderate to high	Low (only during impact)
Seismic resistance originates from:	Appreciable strength and ductility	Low strength and low stiffness in association with the capability to accommodate large displacements	Low to moderate strength and appreciable **rotational inertia**
Equivalent static lateral force analysis is applicable?	Yes	Yes	No
Design philosophy	Equivalent Static	Equivalent Static	Dynamic

* Makris and Vassiliou (2011)
† LRB = Lead Rubber Bearings
‡ CSB = Concave Sliding Bearings

2010; Hung et al., 2011; Deng et al., 2012; Gelagoti et al., 2012; among others) either at the bottom of shear walls or even at the foundation level by allowing appreciable rotations of the footings due to eccentric loading. In this way, the seismic resistance of these "hybrid" structural systems originates primarily from the intentional creation of a lower failure mechanism which, once mobilized, reduces the seismic demand on other critical locations of the structure; while, rocking motion in the way that is illustrated in Fig. 3 happens only to some individual members of the overall moment-resisting yielding frame. Consequently, in this class of hybrid systems the development of rotational accelerations of the individual rocking members is somehow suppressed since their motion needs to be compatible with the lateral motion of the overall yielding frame. Accordingly, the seismic resistance of these yielding frames is "in-between" that of a traditional moment-resisting yielding frame and that of a rocking frame. In most cases the ductile behaviour of the overall moment-resisting yielding frame dominates the system behaviour and in this case a "capacity" design approach may be applicable (Gajan et al., 2008).

3. Equation of motion of the free-standing rocking column

For negative rotations ($\theta > 0$), the equation of motion of a rocking column is

$$-m\ddot{u}_g(t)R\cos[-\alpha - \theta(t)] = I_o\ddot{\theta}(t) + mgR\sin[-\alpha - \theta(t)] \qquad \theta < 0 \tag{4}$$

Eqs. (2) and (4) are well known in the literature (Yim et al., 1980; Makris and Roussos, 2000; Zhang and Makris, 2001; and references reported therein) and are valid for arbitrary values of the slenderness angle $\alpha = \arctan(b/h)$. Eqs. (2) and (4) can be expressed in the compact form

$$\ddot{\theta}(t) = -p^2\Big\{\sin\left[\alpha\,\mathrm{sgn}[\theta(t)] - \theta(t)\right] + \frac{\ddot{u}_g}{g}\cos\left[\alpha\,\mathrm{sgn}[\theta(t)] - \theta(t)\right]\Big\} \tag{5}$$

where 'sgn' is the signum function.

In Eq. (5), the quantity $p = \sqrt{mRg/I_o}$ is the frequency parameter of the column and is an expression of its size. For rectangular columns $p = \sqrt{3g/4R}$.

Fig. 3 (bottom) shows the moment–rotation relationship during the rocking motion of a free-standing column. The system has infinite stiffness until the magnitude of the applied moment reaches the value $mgR\sin\alpha$, and once the column is rocking, its restoring force decreases monotonically, reaching zero when $\theta = \alpha$. This negative stiffness, which is inherent in rocking systems, is most attractive in earthquake engineering in terms of keeping base shears and moments low (Makris and Konstantinidis, 2003), provided that the rocking column remains stable, thus the need for a formulae that will offer a safe design value for its slenderness (Makris and Vassiliou, 2012).

During the oscillatory rocking motion, the moment–rotation curve follows the curve shown in Fig. 3 without enclosing any area. Energy is lost only during impact, when the angle of rotation reverses (Housner, 1963).

Following Housner's seminal paper, a number of studies have been presented to address the complex dynamics of one of the simplest man-made structures—the free-standing rigid column. Yim et al. (1980) conducted numerical studies by adopting a probabilistic approach; Aslam et al. (1980) confirmed with experimental studies that the rocking response of rigid columns is sensitive to system parameters, whereas Psycharis and Jennings (1983) examined the uplift of rigid bodies supported on viscoelastic foundation. Subsequent studies by Spanos and Koh (1984) investigated the rocking response due to harmonic steady-state loading and identified 'safe' and 'unsafe' regions together with the fundamental and subharmonic modes of the system. Their study was extended by Hogan (1989; 1990) who further elucidated the mathematical structure of the problem by introducing the concepts of orbital stability and Poincare sections. The steady-state rocking response of rigid columns was also studied analytically and experimentally by Tso and Wong (1989a;b). Their experimental work provided valuable support to the theoretical findings.

Depending on the level and form of the ground acceleration, in association with the interface conditions at the base, a free-standing rigid column may translate with the ground, slide, rock, or slide-rock. Analytical and numerical studies on the possible motions of a rigid body were presented by Ishiyama (1982) and Sinopoli (1989). These studies were followed by Scalia and Sumbatyan (1996) and Shenton (1996), who independently indicated that, in addition to pure sliding and pure rocking, there is a slide-rock mode and its manifestation depends not only on the width-to-height ratio and the static friction coefficient but also on the magnitude of the base acceleration.

4. The dynamics of the rocking frame

While the increasing dynamic stability of a solitary free-standing column as its size increases (large values of ω_p/p) has been documented in a series of publications (Housner, 1963; Yim et al., 1980; Makris and Roussos, 2000; Zhang and Makris, 2001; Acikgoz and DeJong, 2012; among others and references report therein), the concept of rocking isolation becomes attractive and implementable once the dynamics of the rocking frame like the one shown in Fig. 1 (right) or Fig. 2 is delineated and explained to the extent that it can be easily used by design engineers.

In an effort to explain the seismic stability of ancient free-standing columns that support heavy epistyles together with the even heavier frieze atop, Makris and Vassiliou (2013) studied the planar rocking response of an array of free-standing columns capped with a freely supported rigid beam as shown in Fig. 9.

The free-standing rocking frame shown in Fig. 4 is a single degree of freedom (DOF) structure with size $R = \sqrt{b^2 + h^2}$ and slenderness $\alpha = \mathrm{atan}(b/h)$. The only additional parameter that influences the dynamics of the rocking frame is the ratio of the mass of the cap beam, m_b, to the mass of all the N rocking columns, m_c, given by $\gamma = m_b/Nm_c$. For the Temple of Apollo in Corinth where the frieze is missing, γ is as low as 0.3, whereas in prefabricated bridges, $\gamma > 4$. As in the case of the single rocking column, the coefficient of friction is large enough so that sliding does not occur at the pivot point at the base and at the cap beam. Accordingly, the horizontal translation displacement $u(t)$ and the vertical lift $v(t)$ of the cap beam are functions of the single DOF, $\theta(t)$. Following a variational formulation Makris and Vassiliou (2013) showed that the equation of motion of the rocking frame shown in Fig. 4 is

$$\ddot{\theta}(t) = -\frac{1+2\gamma}{1+3\gamma}p^2\Big(\sin\left[\alpha\,\mathrm{sgn}[\theta(t)] - \theta(t)\right] + \frac{\ddot{u}_g(t)}{g}\cos\left[\alpha\,\mathrm{sgn}[\theta(t)] - \theta(t)\right]\Big) \quad (6)$$

Eq. (7), which describes the planar motion of the free-standing rocking frame, is precisely the same as Eq. (5), which describes the planar rocking motion of a single free-standing rigid column with the same slenderness α, except that in the rocking frame, the term p^2 is multiplied by the factor $(1 + 2\gamma)/(1 + 3\gamma)$. Accordingly, the frequency parameter of the rocking frame, $\hat{p}$, is

$$\hat{p} = \sqrt{\frac{1+2\gamma}{1+3\gamma}}\,p \quad (7)$$

where $p = \sqrt{3g/4R}$ is the frequency parameter of the solitary rocking column and $\gamma = m_b/Nm_c$ is the mass of the cap beam to the mass of all N columns.

According to Eq. (7), the rocking response and stability analysis of the free-standing rocking frame with columns having slenderness, α, and size, R, is described by all the past published work on the rocking response of the free-standing single column (Housner, 1963; Yim et al., 1980; Aslam et al., 1980; Ishiyama, 1982; Spanos and Koh, 1984; Zhang and Makris, 2001; Makris and Konstantinidis, 2003; Vassiliou and Makris, 2012; Dimitrakopoulos and DeJong, 2012; among others), where the column has the same slenderness, α, and a larger size, $\hat{R}$, given by

$$\hat{R} = \frac{1+3\gamma}{1+2\gamma}R = \left(1 + \frac{\gamma}{1+2\gamma}\right)R \quad (8)$$

The remarkable result offered by Eq. (7)—that the heavier the cap beam is, the more stable is the free-standing rocking frame despite the rise of the center of gravity of the cap beam—has been also confirmed by the author after obtaining Eq. (7) for a pair of columns with the algebraically intense direct formulation after deriving the equations of motion of the two-column frame through dynamic equilibrium (Makris and Vassiliou, 2014). Furthermore,

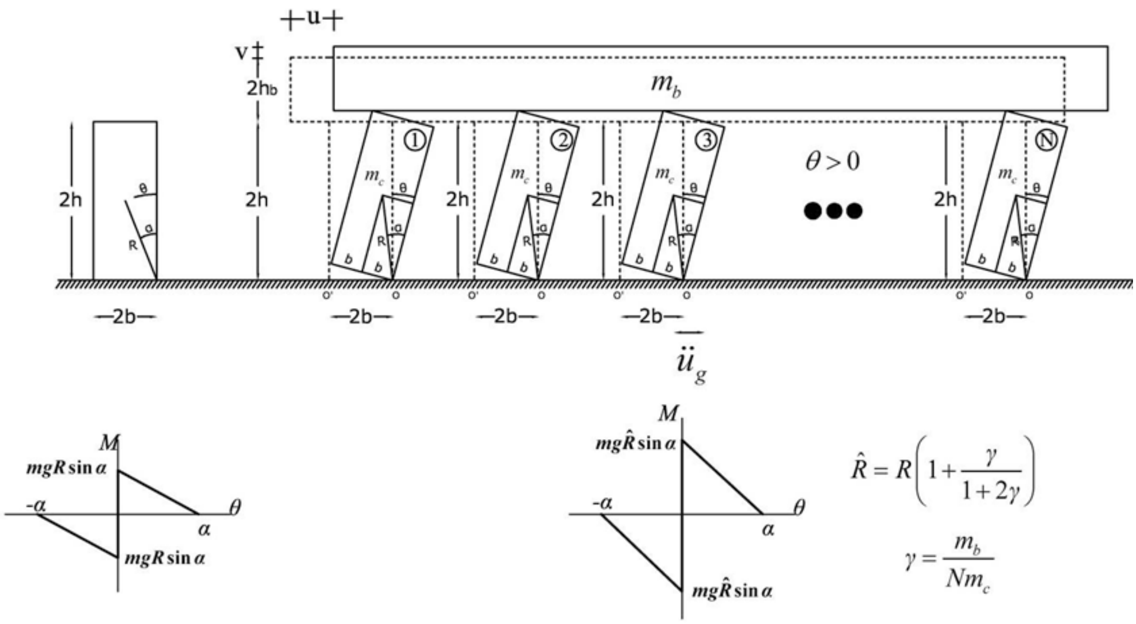

Figure 4: The free-standing rocking frame with columns having size R and slenderness α is more stable than the solitary free-standing column shown on the left having the same size and slenderness.

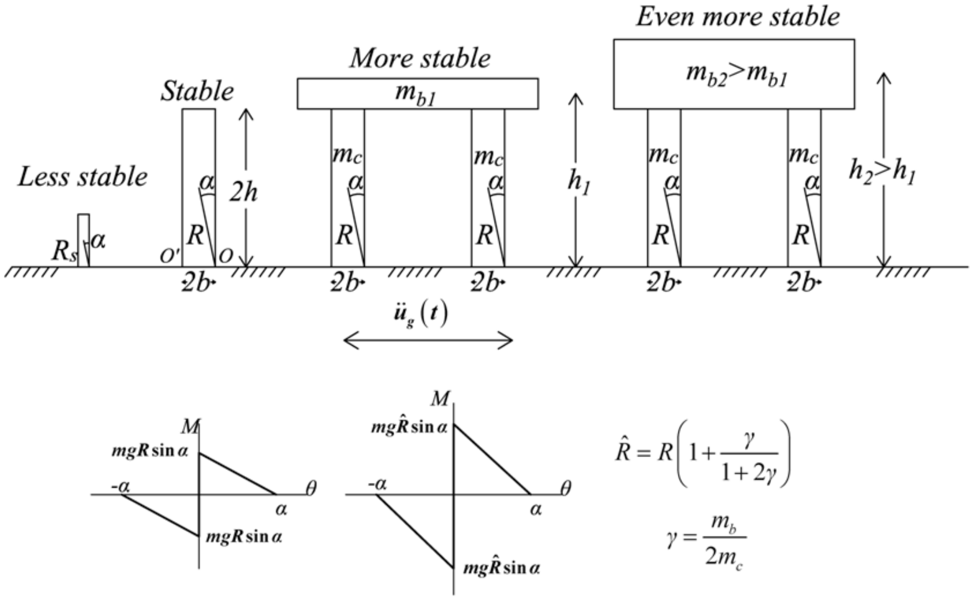

Figure 5: The large free-standing column with size *R* and slenderness *α* is more stable than the geometrically similar smaller column shown at the far left of the figure. The free-standing rocking frame with columns having the same size *R* and same slenderness *α* is more stable than the solitary rocking column. A heavier freely supported cap-beam renders the rocking frame even more stable regardless of the rise of the center of gravity of the system.

numerical studies with the discrete element method by Papaloizou and Komodromos (2009) concluded the same result—that the planar response of free-standing columns supporting epistyles is more stable than the response of the solitary, free-standing column. This finding has also been confirmed in the experimental studies of Mouzakis et al. (2002), and Drosos and Anastasopoulos (2014). Fig. 5 summarizes the increasing seismic stability as we go from the solitary free-standing column to the free-standing rocking frame.

5. The emerging concept of rocking isolation for bridges

The concept of allowing the piers of tall bridges to rock is not new. For instance, the beneficial effects that derive from uplifting and rocking have been implemented since the early 1970's in the South Rangitikei Bridge in New Zealand (Beck and Skinner, 1971). Nevertheless, despite the successful design of the South Rangitikei bridge and the ample dynamic stability of the rocking frame as documented Eq. (6) and further confirmed by numerical and experimental studies (Ishiyama, 1982; Psycharis et al., 2003; Papaloizou and Komodromos, 2009; Mouzakis et al., 2002; Drosos and Anastasopoulos, 2014; Makris, 2014) most modern tall bridges (with tall slender piers) are protected from seismic action via base (shear) isolation of the deck, rather than via (the most natural) rocking isolation. Part of the motivation of this work is to show in the simplest possible way that in the event that a rocking system is selected, the heavy deck atop the tall slender columns not only does not harm the stability of the columns but in contrast enhances the stability of the entire rocking system as shown by Eq. (6).

This work comes to support the emerging design concept (mainly advanced by the prefabricated bridge technology) of concentrating the inelastic deformations of bridge frame at the locations where the bridge piers meet the foundation and the deck (Mander and Cheng. 1997; Sakai and Mahin, 2004; Wacker et al., 2005; Mahin et al., 2006; Cheng, 2008; Cohagen et al., 2008; Yamashita and Sanders, 2009; Barthès et al., 2010; among others). It shall however be stressed that in the prefabricated bridge technology, the bridge piers and the deck are not free-standing, therefore, the structural system is essentially a hybrid system in between the rocking frame examined in this work and a traditional ductile moment-resisting frame.

At present, the equivalent static lateral force procedure is deeply rooted in the design philosophy of the structural engineering community which is primarily preoccupied with how to improve the ductility and performance of the seismic connections; while the ample dynamic rocking stability that derives from the beneficial coexistence of large rotational inertia, negative stiffness and gravity as described by Eq. (6) is ignored. At the same time, it shall be recognized that during the last decade there have been several publications which have voiced the need to go beyond the elastic response spectrum and the associated equivalent static lateral force procedure (Makris and Konstantinidis, 2003; Lagomarsino et al., 2004; Apostolou et al., 2007; Resemini et al., 2008; Anastasopoulos et al., 2010; Dimitrakopoulos and DeJong, 2012; Makris, 2014b; among others). In addition to these studies, Acikgoz and DeJong (2012) and Vassiliou et al. (2013) have examined in depth the rocking response of flexible, slender structures and the main conclusion is that the flexure of a tall rocking structure further increases its seismic stability. To this end, it is worth mentioning the recent theoretical work on the three-dimensional rocking response of free-standing columns (Konstantinidis and Makris, 2007; Zulli et al., 2012; Chatzis and Smyth, 2012a;b) which confirms the seismic stability of free-standing columns in three dimensions. The time is therefore ripe for the development of new, physically motivated alternative seismic protection technology for the design of large, slender structures. Part of the motivation for this work is to bring forward the ample seismic stability associated with the free rocking of large, slender structures and the corresponding rocking frame.

6. Conclusions

Half a century ago George Housner's 1963 seminal paper marked the beginning of a series of systematic studies on the dynamic response and stability of rocking structures which gradually led to the development of rocking isolation—an attractive practical and economical alternative for the seismic protection of tall, slender structures which originates from the mobilization of their large rotational inertia.

After revisiting Housner's size–frequency scale effect for the solitary column which merely explains that when a free-standing column is sufficiently large it can survive any strong shaking, the article builds upon a recent remarkable result—that the dynamic rocking response of an array of free-standing columns capped with a rigid beam is identical to the rocking response of a solitary column with the same slenderness; yet, with larger size, which is a more stable configuration (Eq. 6). Most importantly, the dynamics of the rocking frame reveals that the heavier the freely supported beam is, the more stable is the rocking frame regardless of the rise of the center of gravity of the cap beam, concluding that top-heavy rocking frames are more stable than when they are top-light.

This "counterintuitive" behaviour renders rocking isolation a most attractive alternative for the seismic protection of bridges given that the heavier is the deck, the more stable is the rocking bridge. The realization of a truly rocking frame which can fully mobilize its rotational inertia with neither post-tensioning nor continuation of the longitudinal reinforcement through the rocking interfaces shall remove several of the failure mechanisms associated with the seismic connections of prefabricated bridges such as buckling and fracture of the longitudinal reinforcing bars or spallings of the concrete corners.

Acknowledgments

Partial financial support for this work has been provided by the research project "SeismoRockBridge" which is implemented under the "ARISTEIA" Action of the "OPERATIONAL PROGRAMME EDUCATION AND LIFELONG LEARNING" and is co-funded by the European Social Fund (ESF) and Greek National Resources. The recent distinguished visiting fellowship (DVF1415/2/53) that was awarded to the author by the Royal Academy of Engineering under the Newton Research Collaboration program to lecture at British Universities on this technical subject is also appreciated. The author wishes to thank Professor Andreas Kappos from the City University, London for hosting his visit in the UK.

References

Acikgoz, S., & DeJong, M. J. (2012). The interaction of elasticity and rocking in flexible structures allowed to uplift. *Earthquake Engineering & Structural Dynamics*, **41:** 2177–2194.

Ajrab, J., Pekcan, G., & Mander, J. (2004). Rocking wall–frame structures with supplemental tendon systems. *Journal of Structural Engineering*, **130:** 895–903.

Anastasopoulos, I., Gazetas, G., Loli, M., Apostolou, M., & Gerolymos, N. (2010). Soil failure can be used for seismic protection of structures. *Bulletin of Earthquake Engineering*, **8:** 309–326.

Apostolou, M., Gazetas, G., Garini, E. (2007). Seismic response of slender rigid structures with foundation uplift. *Soil Dynamics and Earthquake Engineering*, **27:** 642–654.

Aslam, M., Scalise, D. T., & Godden, W. G. (1980). Earthquake rocking response of rigid blocks. *Journal of the Structural Engineering Division (ASCE)*, **106:** 377–392.

Barthès, C., Hube, M., & Stojadinović, B. (2010). Dynamics of post-tensioned rigid blocks. *9th US & 10th Canadian Conference on Earthquake Engineering*, Toronto, Canada.

Beck, J. L., & Skinner, R. I. (1974). The seismic response of a reinforced concrete bridge pier designed to step. *Earthquake Engineering & Structural Dynamics*, **2:** 343–358.

Chatzis, M. N., & Smyth, A. W. (2012a). Modeling of the 3D rocking problem. *International Journal of Non-Linear Mechanics*, **47:** 85–98.

Chatzis, M. N., & Smyth, A. W. (2012b). Robust modeling of the rocking problem. *Journal of Engineering Mechanics*, **138:** 247–262.

Cheng, C.-T. (2008). Shaking table tests a self-centering designed bridge substructure. *Engineering Structures*, **30:** 3426–3433.

Cohagen, L., Pang, J. B. K., Stanton, J. F., & Eberhard, M. O. (2008). A precast concrete bridge bent designed to recenter after an earthquake. *Research report*, Federal Highway Administration.

Deng, L., Kutter, B., & Kunnath, S. (2012). Centrifuge modeling of bridge systems designed for rocking foundations. *Journal of Geotechnical and Geoenvironmental Engineering*, **138:** 335–344.

Dimitrakopoulos, E. G., & DeJong, M. J. (2012). Revisiting the rocking block: closed-form solutions and

similarity laws. *Proceedings of the Royal Society A*, **468:** 2294–2318.
Drosos, V., & Anastasopoulos, I. (2014). Shaking table testing of multidrum columns and portals. *Earthquake Engineering & Structural Dynamics*. **43:** 1703–1723.
Gajan, S., Hutchinson, T. C., Kutter, B. L., Raychowdhury, P., Ugalde, J. A., & Stewart, J. P. (2008). Numerical models for analysis and performance-based design of shallow foundations subject to seismic loading. *Report No. PEER-2007/04*, Pacific Earthquake Engineering Research Center, University of California, Berkeley.
Gajan, S., & Kutter, B. (2008). Capacity, settlement, and energy dissipation of shallow footings subjected to rocking. *Journal of Geotechnical and Geoenvironmental Engineering,* **134:** 1129–1141.
Gelagoti, F., Kourkoulis, R., Anastasopoulos, I., & Gazetas, G. (2012). Rocking isolation of low-rise frame structures founded on isolated footings. *Earthquake Engineering & Structural Dynamics*, **41:** 1177–1197.
Harden, C., Hutchinson, T., & Moore, M. (2006). Investigation into the effects of foundation uplift on simplified seismic design procedures. *Earthquake Spectra,* **22:** 663–692.
Hogan, S. J. (1989). On the dynamics of rigid-block motion under harmonic forcing. *Proceedings of the Royal Society A*, **425:** 441–476.
Hogan, S. J. (1990). The many steady state responses of a rigid block under harmonic forcing. *Earthquake Engineering & Structural Dynamics,* **19:** 1057–1071.
Housner, G. W. (1963). The behaviour of inverted pendulum structures during earthquakes. *Bulletin of the Seismological Society of America*, **53:** 404–417.
Hung, H.-H., Liu, K.-Y., Ho, T.-H., & Chang, K.-C. (2011). An experimental study on the rocking response of bridge piers with spread footing foundations. *Earthquake Engineering & Structural Dynamics*, **40:** 749–769.
Ikegami, R., & Kishinouye, F. (1947). A study on the overturning of rectangular columns in the case of the Nankai earthquake on December 21, 1946. *Bulletin of the Earthquake Research Institute, University of Tokyo,* **25:** 49–55.
Ikegami, R., & Kishinouye, F. (1950). The acceleration of earthquake motion deduced from overturning of the gravestones in case of the Imaichi Earthquake on Dec. 26, 1949. *Bulletin of the Earthquake Research Institute, University of Tokyo,* **28:** 121–128.
Ishiyama, Y. (1982). Motions of rigid bodies and criteria for overturning by earthquake excitations. *Earthquake Engineering & Structural Dynamics,* **10:** 635–650.
Kawashima, K., Nagai, T., & Sakellaraki, D. (2007). Rocking Seismic Isolation of Bridges Supported by Spread Foundations. *Proceedings of the 2nd Japan-Greece Workshop on Seismic Design, Observation and Retrofit of Foundations*, Japan Society of Civil Engineers, Tokyo, Japan, **2:** 254–265.
Kirkpatrick, P. (1927). Seismic measurements by the overthrow of columns. *Bulletin of the Seismological Society of America*, **17:** 95–109.
Konstantinidis, D., & Makris, N. (2007). The Dynamics of a rocking block in three dimensions. *Proceedings of the 8th HSTAM International Congress on Mechanics*, Patras, Greece.
Lagomarsino, S., Podestà, S., Resemini, S., Curti, E., & Parodi, S. (2004). Mechanical models for the seismic vulnerability assessment of churches. *Proceedings of IV SAHC*, Padova, Italy, **2:** 1091–1101.
Mahin, S., Sakai, J., & Jeong, H. (2006). Use of partially prestressed reinforced concrete columns to reduce post-earthquake residual displacements of bridges. *Proceedings of the 5th National Seismic Conference on Bridges & Highways*, San Francisco.
Makris, N., & Roussos, Y. (1998). Rocking response and overturning of equipment under horizontal pulse-type motions. *Rep. No. PEER-98/05*, Pacific Earthquake Engineering Research Center, University of California, Berkeley, California
Makris, N., & Roussos, Y. (2000). Rocking response of rigid blocks under near-source ground motions. *Geotechnique*, **50:** 243–262.
Makris, N., & Konstantinidis, D. (2003). The rocking spectrum and the limitations of practical design methodologies. *Earthquake Engineering & Structural Dynamics,* **32:** 265–289.
Makris, N., & Vassiliou, M. F. (2013). Planar rocking response and stability analysis of an array of free-standing columns capped with a freely supported rigid beam. *Earthquake Engineering & Structural Dynamics*, **42:** 431–449.
Makris, N., & Vassiliou, M. F. (2014). *Are some top-heavy structures more stable?* Journal of Structural Engineering, **140**.
Makris, N. (2014a). The role of the rotational inertia on the seismic resistance of free-standing rocking columns and articulated frames. *Bulletin of the Seismological Society of America*, **104:** 2226–2239.
Makris, N. (2014b). A half century of rocking isolation. *Earthquakes and Structures*, **7:** 1187–1221.
Mander, J. B., & Cheng, C.-T. (1997). Seismic resistance of bridge piers based on damage avoidance design, *Tech. Rep. No. NCEER-97-0014*, National Center for Earthquake Engineering Research, Dept. of Civil and Environmental Engineering, State Univ. of New York, Buffalo, N.Y.
Milne, J. (1885). Seismic experiments. *Transactions of the Seismological Society of Japan,* **8:** 1–82.
Mouzakis, H. P., Psycharis, I. N., Papastamatiou, D. Y., Carydis, P. G., Papantonopoulos, C., & Zambas, C. (2002). Experimental investigation of the earthquake response of a model of a marble classical column. *Earthquake Engineering & Structural Dynamics*, **31:** 1681–1698.

Muto, K., Umemure, H., & Sonobe, Y. (1960). Study of the overturning vibration of slender structures. *Proceedings of the 2nd World Conference on Earthquake Engineering*, Japan, 1239–1261.

Papaloizou, L., & Komodromos, K. (2009). Planar investigation of the seismic response of ancient columns and colonnades with epistyles using a custom-made software. *Soil Dynamics and Earthquake Engineering*, **29:** 1437–1454.

Powell B. (1905). The Temple of Apollo Corinth. *American Journal of Archaeology*, **9:** 44–63.

Psycharis, I. N., & Jennings, P. C. (1983). Rocking of slender rigid bodies allowed to uplift. *Earthquake Engineering & Structural Dynamics*, **11:** 57–76.

Psycharis, I. N., Lemos, J. V., Papastamatiou, D. Y., & Zambas, C. (2003). Numerical study of the seismic behaviour of a part of the Parthenon Pronaos. *Earthquake Engineering & Structural Dynamics*, **32:** 2063–2084.

Resemini S., Lagomarsino, S. & Cauzzi, C. (2008). Dynamic response of rocking masonry elements to long period strong ground motion. *Proceedings of the 14th World Conference on Earthquake Engineering*, Beijing, China.

Sakai, J., & Mahin, S. (2004). Analytical investigations of new methods for reducing residual displacements of reinforced concrete bridge columns. *PEER Report 2004/02*, Pacific Earthquake Engineering Research Center, University of California, Berkeley, California.

Sinopoli, A. (1989). Kinematic approach in the impact problem of rigid bodies. *Applied Mechanics Reviews (ASME)*, **42:** 233–244.

Spanos, P. D., & Koh, A. S. (1984). Rocking of rigid blocks due to harmonic shaking. *Journal of Engineering Mechanics (ASCE)*, **110:** 1627–1642.

Tso, W. K., & Wong, C. M. (1989a). Steady state rocking response of rigid blocks, Part 1: Analysis. *Earthquake Engineering & Structural Dynamics*, **18:** 89–106.

Tso, W. K., & Wong, C. M. (1989b). Steady state rocking response of rigid blocks, Part 2: Experiment. *Earthquake Engineering & Structural Dynamics,* **18:** 107–120.

Vassiliou, M. F., & Makris, N. (2012). Analysis of the rocking response of rigid blocks standing free on a seismically isolated base. *Earthquake Engineering & Structural Dynamics,* **41:** 177–196.

Vassiliou, M. F., Mackie, K. R., & Stojadinović, B. (2013). Rocking response of slender, flexible columns under pulse excitation. *Proceedings of the 4th ECCOMAS Thematic Conference on Computational Methods in Structural Dynamics and Earthquake Engineering*, Kos Island, Greece, Paper No. C 1084.

Wacker, J. M., Hieber, D. G., Stanton, J. F., & Eberhard, M. O. (2005). Design of precast concrete piers for rapid bridge construction in seismic regions. *Research Report*, Federal Highway Administration

Yamashita, R., & Sanders, D. (2009). Seismic performance of precast unbonded prestressed concrete columns. *ACI Structural Journal*, **106:** 821–830.

Yim, C. S., Chopra, A. K., & Penzien, J. (1980). Rocking response of rigid blocks to earthquakes. *Earthquake Engineering & Structural Dynamics*, **8:** 565–587.

Zhang, J., & Makris, N. (2001). Rocking response of free-standing blocks under cycloidal pulses. *Journal of Engineering Mechanics (ASCE)*, **127:** 473–483.

Zulli, D., Contento, A., & Di Egidio, A. (2012). 3D model of rigid block with a rectangular base subject to pulse-type excitation. *International Journal of Non-Linear Mechanics*, **47:** 679–687.

Notable Earthquakes March 2014 – April 2014

Reported by British Geological Survey

Issued by: Davie Galloway, British Geological Survey, February 2015.
Non British Earthquake Data supplied by The United States Geological Survey.

Year	Day	Mon	Time UTC	Lat	Lon	Dep km	Magnitude ML	Mb	Mw	Location
2014	01	MAR	13:58	56.85N	7.51E	10	3.2			EASTERN NORTH SEA
2014	02	MAR	20:11	27.43N	127.37E	119			6.5	RYUKYU ISLANDS, JAPAN
2014	03	MAR	17:50	53.21N	1.04W	1	1.6			NEW OLLERTON, NOTTS
Felt New Ollerton (3 EMS).										
2014	10	MAR	02:21	53.21N	1.02W	1	1.8			NEW OLLERTON, NOTTS
Felt New Ollerton (3 EMS).										
2014	10	MAR	05:18	40.83N	125.13W	17			6.8	NORTHERN CALIFORNIA
2014	11	MAR	11:37	53.21N	1.02W	1	1.8			NEW OLLERTON, NOTTS
Felt New Ollerton (3 EMS).										

Year	Day	Mon	Time	Lat	Lon	Dep	Magnitude			Location
			UTC			km	ML	Mb	Mw	
2014	16	MAR	21:16	19.98S	70.70W	20			6.7	TARAPACA, CHILE
2014	18	MAR	20:45	52.32N	6.30W	9	2.2			COUNTY WEXFORD, IRELAND
Felt County Wexford (3 EMS).										
2014	19	MAR	19:34	53.20N	1.02W	1	1.8			NEW OLLERTON, NOTTS
Felt New Ollerton (3 EMS).										
2014	21	MAR	13:45	53.22N	1.02W	1	1.6			NEW OLLERTON, NOTTS
Felt New Ollerton (3 EMS).										
2014	23	MAR	11:46	53.21N	1.02W	1	1.6			NEW OLLERTON, NOTTS
Felt New Ollerton (3 EMS).										
2014	25	MAR	04:23	53.21N	1.02W	1	1.7			NEW OLLERTON, NOTTS
Felt New Ollerton (3 EMS).										
2014	30	MAR	13:29	53.21N	1.02W	1	1.6			NEW OLLERTON, NOTTS
Felt New Ollerton (3 EMS).										
2014	01	APR	23:46	19.61S	70.77W	25			8.2	TARAPACA, CHILE
Six people killed, scores more injured and at least 2,500 buildings and 150 boats damaged in the Iquique area, Tarapaca. Many landslides and power outages also occurred in the epicentral area. A tsunami was also generated with a maximum wave height of 87cm recorded at Tocopilla, Chile.										
2014	01	APR	23:57	19.89S	70.95W	28			6.9	TARAPACA, CHILE
2014	03	APR	01:58	20.31S	70.58W	24			6.5	TARAPACA, CHILE
2014	03	APR	02:43	20.57S	70.49W	22			7.7	TARAPACA, CHILE
2014	03	APR	06:30	51.72N	2.25W	16	2.3			STROUD, GLOUCESTERSHIRE
Felt Stroud (2 EMS).										
2014	04	APR	22:40	28.17N	103.62E	25		5.4		YUNNAN, CHINA
At least 21 people injured, 75 houses destroyed and 2,700 others damaged in the Yongshan area of Yunnan Province, China.										
2014	11	APR	07:07	6.59S	155.05E	61			7.1	PAPUA NEW GUINEA
One person killed and at least 50 buildings destroyed in the town of Buin on Bougainville Island, PNG.										
2014	11	APR	08:16	6.79S	154.95E	20			6.5	PAPUA NEW GUINEA
2014	11	APR	20:29	11.64N	85.88W	135			6.6	NICARAGUA
2014	12	APR	20:14	11.27S	162.15E	23			7.6	SOLOMON ISLANDS
2014	13	APR	12:36	11.46S	162.05E	39			7.4	SOLOMON ISLANDS
2014	13	APR	13:24	11.13S	162.05E	10			6.6	SOLOMON ISLANDS
2014	15	APR	03:57	53.50S	8.72E	11			6.8	BOUVET ISLAND REGION
2014	17	APR	06:07	52.73N	0.73W	2	3.2			OAKHAM, RUTLAND
Felt throughout Rutland, Leicestershire and surrounding areas (4 EMS).										
2014	18	APR	06:50	52.72N	0.73W	3	3.5			OAKHAM, RUTLAND
Felt throughout Rutland, Leicestershire and surrounding areas (4 EMS).										
2014	18	APR	14:27	17.40N	100.97W	24			7.2	GUERRERO, MEXICO
2014	19	APR	01:04	6.66S	155.09E	29			6.6	PAPUA NEW GUINEA
2014	19	APR	13:28	6.76S	155.02E	43			7.5	PAPUA NEW GUINEA
2014	24	APR	03:10	49.64N	127.73W	10			6.5	VANCOUVER ISLAND, CANADA
2014	28	APR	22:05	52.72N	0.73W	3	1.7			OAKHAM, RUTLAND
Felt Oakham, Cottesmore, Ashwell, Langham and Braunston, Rutland (3 EMS).										